Model of intermittency in three-dimensional turbulence

Eric D. Siggia
Department of Physics, University of Pennsylvania, Philadelphia, Pennsylvania 19174
and National Center for Atmospheric Research, Post Office Box 3000, Boulder, Colorado 80307
(Received 28 November 1977)

A double decomposition of phase space into both wave-number bands and spacially localized wave packets is used to derive model equations for an averaged time-dependent velocity or vorticity amplitude localized in both real and Fourier space. Intermittency develops in time, and correlation functions scale as the wave number to a universal power. Energy cascades to infinite wave number in a finite time in a series of self-similar pulses that propagate down our hierarchy of equations. A number of subgrid parametrizations are also examined.

I. INTRODUCTION

The most common means of measuring intermittency in high-Reynolds-number flows are experiments employing a single hot-wire anemometer in the atmosphere.[1] These measurements, together with Taylor's observation that for the small scales convection frequencies exceed intrinsic eddy turnover frequencies, imply the spacial spottiness associated with intermittency. It is our contention that intermittency can equivalently be viewed as a temporal phenomena for appropriately chosen variables.[2] It is not easy to give a precise mathematical definition of these variables, and their utility is dependent upon a number of commonly accepted, but unproven, properties of fully developed homogeneous isotropic turbulence in three dimensions.[3]

The theory developed here is dynamical in that it utilizes a hierarchy of differential equations in time to model the buildup of intermittency in the inertial range. We believe that intermittency is a consequence of inertial range dynamics[4] and for this reason prefer Van Atta's time-differencing treatment of the atmospheric data because it directly produces the probability distribution of velocity fluctuations for a given scale size.[5] The more conventional data reduction, that displays locally averaged dissipation spectra, contains the same information but in a form less convenient for comparison with an inertial range theory.

It will prove useful in what follows to imagine Fourier space partitioned into bands or shells on a logarithmic scale. The nth shell will consist of all wave numbers k satisfying

$$b^n \leq k < b^{n+1} ,$$

where b is a number of order 2, and units have been chosen to make the largest eddies in the system fall into the zeroth shell. It is generally believed that the energy cascade in three dimensions is local in wave number, with the intrinsic coupling (i.e., with convection effects removed) between shells m and n decreasing exponentially with $|n-m|$.[6] Estimates based on second-order closures indicate that most of the energy transfer into a shell comes from a range of about 10 in wave number.[6] In the model of Ref. 2, only interactions between neighboring bands were permitted for numerical simplicity. Energy was still conserved at every instant and we are inclined to believe such an approximation is qualitatively correct. We continue to make this assumption in the highly simplified model that is solved here.

Closure calculations for homogeneous isotropic turbulence are commonly done in k space. Fourier modes, however, are not well suited for describing a process which becomes spotty in real space. A real-space representation would be closer to experiment, but apart from the impossibility of doing a direct simulation of the small scales at high Reynolds number, the pressure term is spacially nonlocal and is much easier to compute in Fourier space.

An obvious, though imprecise, way of reconciling these conflicting requirements on the basis functions are the wave packets introduced in Ref. 2.[7] Briefly, one imagines reexpressing the modes in a given wave number band n in terms of functions $\phi_{n,G}(r-R_{n,\alpha}(t))$ which are localized to a region of characteristic size $2\pi \times 2^{-n}$ ($b=2$) about R_α. The region was taken to be a cube to facilitate numerical calculations. For each n, there are sufficient $R_{n,\alpha}$ so that the corresponding cubes fill all space. Within each cube and multiplying the "top-hat" function, are Fourier modes, $\exp(i\vec{G}\cdot\vec{r}2^n)$, where $\vec{G}$ is a vector with components 0, ±1 and magnitude between 1 and $\sqrt{3}$.

If one expands the band velocity u_n,

$$u_n(r,t) = \sum_{G,\alpha} A_G^{n,\alpha}(t)\phi_{n,G}(r-R_{n,\alpha}(t)) ,$$

and substitutes into the Navier-Stokes equations, the crude estimates in Ref. 2 suggest that the intraband interactions of the $A_G^{n,\alpha}$ are predominantly with modes in the same box. The incompressibility constraint is satisfied separately within each cube. Physically, this corresponds to the assertion that spacially distinct eddies of the same characteristic size do not interact. The center of each cube is time dependent since we wish to follow only the proper motions in a given shell and therefore let $R_\alpha(t)$ evolve with the local spacially averaged velocity of the preceding shells. We are thus working in local Lagrangian coordinates. The transformation to coordinates that describe the eddies of given characteristic size in a given comoving region itself evolves in time. Except for trivial convection effects, it should be faithful for at least a local eddy turnover time which is all that is really needed.

The modes $A_{G,\alpha}^n$ correspond to velocity differences over a region of size $2\pi \times 2^{-n}$, filtered to remove fluctuations on much smaller scales. Interactions between modes in different shells are generated when the corresponding basis functions overlap. We believe that for each α, each set of $A_{G,\alpha}^n$, with n fixed, are statistically equivalent, and that a time average for a fixed α or box would be the same as a spacial average over all the boxes in a given shell at a single time.[2]

Until now, our new basis might be considered exact though useless, since it has the same number of degrees of freedom as the nth shell. To make progress, the number of modes used to represent a given shell is reduced by retaining only one box with its 26 Fourier modes $\vec{G}$. We continue to assume that statistical properties can be computed as time averages. This approximation tends to increase the intermittency since it omits the spacial diffusion of energy within a band.[4] The intershell coupling is calculated by nesting the boxes representing successive shells.

When the scheme we have outlined was implemented in Ref. 2, intermittency appeared as bursts of activity in time. The energy transfer was small for comparatively long periods, but fluctuated well above its mean for short periods so as to maintain a statistically stationary distribution. A Kolmogorov spectrum developed for the energy with the suggestion of a small positive correction to $\frac{5}{3}$.[1] The variance of the energy transfer rate, that we assume to be analogous to the variance of the locally averaged dissipation spectrum or the structure function $\langle [v(r)-v(0)]^6\rangle/r^2$,[5] scaled with r and give a value of μ of order 0.8. We emphasize that these calculations were designed only to check that the generally accepted characteristics of high-Reynolds-number flows lead to fluctuation effects qualitatively like experiment.

A model with 26 Fourier modes per band still requires a moderate amount of computer time to solve. A much simpler model is studied here with only one variable per band whose solution proves to be very similar to that of the more complicated model. It is rather like a model of a model since the one variable corresponds to an average of $|\vec{A}_{G,\alpha}^n|$ over $\vec{G}$. The present model is complementary to the earlier one, since it contains a number of arbitrary constants whose signs we are able to infer from the more realistic model. It permits us, however, to investigate a number of effects that would have been too complicated to treat with 78 ($=3\times 26$) variables per band.

Section II contains a statement of our model and its relation to the Navier-Stokes equations and the model of Ref. 2. A stationary solution of the model is found that can plausibly be identified with Kolmogorov's 1941 theory.[3] The stability properties of this solution are examined in Sec. III. Finally, in the parameter regime in which $K41$ is unstable, numerical solutions of the nonlinear equations are given. From their form the exponents relating to fluctuations in the energy transfer rate and corrections to the "$\frac{5}{3}$" law can be found. In the conclusion, we discuss a number of alternative theories of intermittency; in particular, the prevalent viewpoint that intermittency is due to the convection of comparatively stable large-scale convoluted structures.[8,9]

II. DEFINITION OF MODEL

For a cascade model involving only interactions between nearest-neighbor bands and conserving the modal energy $E_n=\frac{1}{2}\sum_G|\vec{A}_G^n|^2$, at each instant, one can write[2]

$$\frac{dE_n}{dt}=\epsilon_n-\epsilon_{n+1}. \tag{2.1}$$

The index α has been omitted on A_G^n since we are retaining only one box per shell. The energy entering shell n from $n-1$ is denoted by ϵ_n; and for a statistically stationary and necessarily driven system, the temporal average of ϵ_n is independent of n:

$$\epsilon=\langle\epsilon_n\rangle. \tag{2.2}$$

In Ref. 2, ϵ_n was the sum of a term with factors $[u_n u_{n-1} u_n]$ and one with factors $[u_n u_{n-1} u_{n-1}]$. The brackets stand for a sum of amplitudes A_G^m from the indicated bands together with a projection operator for the pressure and a gradient. Both terms were almost always positive as a function of time, corresponding to energy transfer to small scales. To reduce the number of modes to one per shell, the

obvious choice is to define $E_n=\frac{1}{2}x_n^2$ and set

$$\epsilon_n=b^n(\beta x_{n-1}^2|x_n|+|x_{n-1}|x_n^2). \tag{2.3}$$

This approximation assumes that ϵ_n responds instantly to any change in x_{n-1} or x_n. The factor b^n is simply the magnitude of the average wave vector in the nth shell. In Ref. 2, ϵ_n was an analytic function of the amplitudes A_G^m and was generally positive because of vortex stretching effects. With only one mode per level this physical mechanism is lost and the absolute values are required in (2.3) to enforce the positivity. An overall constant in (2.3) has been absorbed into the time scale and the one remaining parameter β must be taken as positive. The second term in (2.3) models the vortex stretching or the shearing of small scales by larger ones.

The equations we actually integrated were slightly more complicated than (2.3) would imply:

$$\dot{x}_1=\frac{\epsilon}{x_1}-b^2\left(\frac{\beta x_1 x_2^2}{(x_2^2+\alpha x_3^2)^{1/2}}+\frac{x_2^2 x_1}{(x_1^2+\alpha x_2^2)^{1/2}}\right), \tag{2.4a}$$

$$\dot{x}_n=b^n\left(\frac{\beta x_{n-1}^2 x_n}{(x_n^2+\alpha x_{n+1}^2)^{1/2}}+\frac{x_{n-1}^2 x_n}{(x_{n-1}^2+\alpha x_n^2)^{1/2}}\right)$$

$$-b^{n+1}\left(\frac{\beta x_n x_{n+1}^2}{(x_{n+1}^2+\alpha x_{n+2}^2)^{1/2}}+\frac{x_n x_{n+1}^2}{(x_n^2+\alpha x_{n+1}^2)^{1/2}}\right) \tag{2.4b}$$

for $n=2,3,\ldots,N$ and,

$$x_{N+1}=x_N/b^{1/3}, \tag{2.4c}$$

$$x_{N+2}=x_{N+1}/b^{1/3}. \tag{2.4d}$$

Equation (2.4b) implies

$$\epsilon_n=b^n\left(\frac{\beta x_{n-1}^2 x_n^2}{(x_n^2+\alpha x_{n+1}^2)^{1/2}}+\frac{x_{n-1}^2 x_n^2}{(x_{n-1}^2+\alpha x_n^2)^{1/2}}\right). \tag{2.5}$$

The square-root factor has been introduced into (2.4) to smooth out the absolute value and facilitate the numerical integrations. The radicand was selected to preserve the scaling properties of (2.4) as well as the solution (3.1). The parameter α was varied from 10^{-4} to 10^{-2} without significantly affecting the results. The inclusion of an extra parameter actually makes the universality properties of the model more interesting as we discuss in the conclusion.

The first term in the equation for x_1 is designed to feed energy into the system at a constant rate ϵ. Equation (2.2) will hold if (2.4) proves to be statistically stationary. The time scale is set by ϵ and the length scale by $b\sim 2$. Note that the mth equation in (2.4b) is invariant to a change in sign of x_m. A variant of (2.4a) was sometimes used which, except for a scale change, did not alter the results for shells beyond the first few:

$$\dot{x}_1=b\left(\frac{\beta x_0^2 x_1}{(x_1^2+\alpha x_2^2)^{1/2}}+\frac{x_0 x_1}{(1+\alpha)^{1/2}}\right)$$

$$-b^2\left(\frac{\beta x_1 x_2^2}{(x_2^2+\alpha x_3^2)^{1/2}}+\frac{x_1 x_2^2}{(x_1^2+\alpha x_2^2)^{1/2}}\right), \tag{2.6}$$

where x_0 is a constant of order $[\epsilon/(\beta b^{2/3}+b^{1/3})]^{1/3}$. Physically, (2.6) models a constant shear.

We have terminated the system of equations (2.4) with an eddy damping (2.4c), rather than a true viscosity. This is because Desnyansky and Novikov[10] have shown for $\beta=\alpha=0$ that (2.4) with a damping term, $-b^{2n}x_n/R$, where R is the Reynolds number, does not possess a stationary solution with a Kolmogorov inertial range that is independent of R as $R\to\infty$. We believe this to be an artifact of a model as simple as ours. With an eddy damping, we do obtain a stationary solution corresponding to a $\frac{5}{3}$-law inertial range though of course no dissipation range.

Two more complicated "subgrid" truncations were used in place of (2.4c),[11]

$$\dot{x}_{N+1}=(-x_{N+1}+x_N/b^{1/3})/\tau, \tag{2.7a}$$

which for a statistically stationary system becomes

$$x_{N+1}(t)=b^{-1/3}\int_{-\infty}^{t}e^{-(t-t')/\tau}x_N(t')d\left(\frac{t'}{\tau}\right); \tag{2.7b}$$

and

$$x_{N+1}(t)=x_N(t-\tau)/b^{1/3}. \tag{2.8}$$

Their properties are discussed in Secs. III and IV. A continuum limit of (2.4) is described in the Appendix.

III. STABILITY ANALYSIS

Static solutions to (2.4) can be found by solving

$$\epsilon=\epsilon_n.$$

The most interesting such solution is

$$x_n=\pm cb^{-n/3}, \tag{3.1}$$

where $c=[(1+\alpha/b^{2/3})^{1/2}\epsilon/(\beta b^{2/3}+b^{1/3})]^{1/3}$. Equation (3.1) is equivalent to a $\frac{5}{3}$-law inertial range. Using (2.6) in place of (2.4a) changes only c in (3.1).

The stability properties of (2.4) have been studied numerically as a function of b, α, β, N, and the lag time τ in (2.7) and (2.8). Time dependent solutions of (2.4) are not physically precluded because $\frac{1}{2}x_n^2$ represents the energy in a spacially localized region. The equal time velocity correlation function in k space that occurs in a closure calculation, however, still represents a volume average and cannot fluctuate in a statistically stationary driven system.

The case $\alpha=0$ and $b\simeq 2$ has been examined in most detail. With the substitution, $x_n = cb^{-n/3}(1+\xi_n)$, ξ_n small, the eigenvalue problem corresponding to (2.4) becomes after some rescaling

$$\dot{\xi}_1 = -b^{2/3}[\xi_1 + 2\xi_2 + \beta b^{1/3}(2\xi_1+\xi_2)], \tag{3.2a}$$

$$\dot{\xi}_n = b^{2n/3}[\xi_{n-1}+\xi_n-2\xi_{n+1}+\beta b^{1/3} \times(2\xi_{n-1}-\xi_n-\xi_{n+1})], \quad n=2,3,\ldots,N \tag{3.2b}$$

$$\xi_{N+1}\equiv\xi_N. \tag{3.2c}$$

For $N\geq 4$ and β sufficiently small, (3.2) has at least one eigenvalue with a positive real part indicating that (3.1) is unstable. For $N=8$, 20, and 40 and $b=2$, complete sets of eigenfunctions and eigenvalues were generated numerically as a function of β. All eigenvalues were complex and occurred in complex conjugate pairs. For any $\beta\geq 0$, the first eigenvalue pair has a negative real part for (3.2a) and a positive real part when (2.6) was used for $\dot{x}_1$. The replacement of (2.4a) by (2.6) only affected the lowest few eigenvalues. As β approached $\beta^*=0.150\,579\,218\,64$ from below, the real parts of the next two pairs of eigenvalues went from positive to negative. The real parts of the remaining $N-6$ eigenvalues all went to zero simultaneously at the value of β^* just given. Furthermore, β^* was independent of N to the accuracy stated. We have no physical explanation for this rather curious fact. When α is nonzero, however, the $N-6$ eigenvalues with largest real parts pass through zero successively but in a very narrow range of β.

Equation (3.2) is tridiagonal and its elements increase as $b^{2n/3}$ along the diagonal, so it is not surprising that the nth eigenvalue is of order $z_n b^{2n/3}$, where z_n is a complex number of order 1. Its eigenvector for $\beta\ll\beta^*$ is localized in k space around the mode n, Fig. 1. The tail that is apparent on the third eigenfunction decreases with N for a fixed eigenvalue. When $\beta\to\beta^*$, these tails grow until at β^*, the mth eigenfunction is spread uniformly over all levels $n\geq m$. The degree of eigenvector localization is a measure of the correlations among the various levels. The Kolmogorov solution becomes stable when the levels are locked together and the eigenfunctions are delocalized.

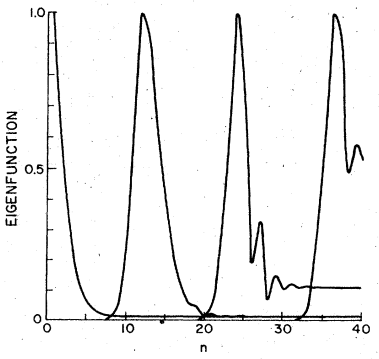

FIG. 1. Eigenfunctions for (2.4) linearized about its stationary solution, (3.1), for $\alpha=\beta=0$, $b=2$, and $N=40$. The corresponding eigenvalues from left to right are in order of magnitude, $b^{2n/3}$, with $n=1, 13, 25$, and 37.

For $\beta<\beta^*$, we have shown that the shells with largest n run away from (3.1) most rapidly. However, near β^*, when all eigenvalues have small real parts, their imaginary parts remain $\sim b^{2n/3}$ so the unstable modes execute a tight spiral around the N-dimensional point $\xi_n=0$ as they grow.

It is also possible to solve for the temporal evolution of the probability distribution in the variables ξ_n when a noise source $\zeta(t)$ satisfying

$$\langle\zeta(t)\zeta(t')\rangle = 2\Gamma\delta(t-t')$$

is added to each equation in (3.2a) and (3.2b). The time evolution matrix in the $\{\xi_n\}$ phase space for a system of equations

$$\dot{\xi}_n = f_n\{\xi\}+\zeta$$

is just a path integral over ξ_n from $\xi_n(0)=\xi_n^{(1)}$ to $\xi_n(T)=\xi_n^{(2)}$ of the expression[12]

$$\prod_{n=1}^{N}\exp\left[-\frac{1}{4\Gamma}\int_0^T\left((\dot{\xi}_n-f_n)^2+2\Gamma\frac{df_n}{dx_n}\right)dt\right].$$

When f_n is linear, the path integral can be evaluated exactly by perturbing about the classical extremal path from $\xi_n^{(1)}$ to $\xi_n^{(2)}$ and doing some linear algebra.[13] The results confirm the conclusions stated above.

The stability problem for (3.2) has been examined in the remainder of the parameter space though in less detail than in the β-N plane. For $\alpha=0.01$ (and presumably for any small or zero α) and for $N=8$ or 20 we found that β^* decreased from a value approximately 1 for b just above 1 to zero at $b\sim 2.75$. Equation (3.1) is a linearly stable solution to (2.4) for $b>2.75$.

For $\alpha=0.01$ complete sets of eigenvalues were again generated. They behaved similarly to those for $\alpha=0$; $\beta^*=0.145\,10$ and $0.145\,26$ for $N=8$ and 20, respectively.

We have also checked the stability properties of (3.2) as α increases. For $\beta=0.05$, Kolmogorov became stable above $\alpha^*=0.122\,86$ and $0.124\,08$ for $N=8$ and 20, respectively. With $\beta=0.0$ and $N=8$, $\alpha^*=0.189\,72$.

The influence of the first subgrid parametrization, (2.7a), on the stability of the Kolmogorov solution has also been checked. Figure 2 shows the regions of instability in the β-τ plane. The initial decrease of β^* with τ and its subsequent rise can

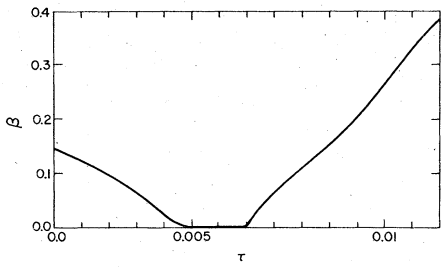

FIG. 2. Curve of β^* vs τ for $\alpha = 10^{-3}$, $b = 2$, and $N = 8$. The solution, (3.1) of Eqs. (2.4a), (2.4b), and (2.7a) is linearly stable (unstable) for $\beta >$ (<) $\beta^*(\tau)$.

best be understood after the nonlinear solutions to (2.4) are examined.

It should be noted that the vortex stretching term

$$x_{n-1}^2 x_n/(x_{n-1}^2 + \alpha x_n^2)^{1/2}$$

in Eq. (2.4b) is responsible for the instability. It causes a small initial x_n to grow exponentially if x_{n-1} is large, while the term proportional to β leads only to algebraic growth. If the time derivative of $\rho = \frac{1}{2}\sum_1^N b^{-2n/3}|\xi_n|^2$ is computed from (3.2), one finds

$$\dot{\rho} = -|\xi_1|^2 - |\xi_N|^2 + \sum_2^{N-1} |\xi_n|^2 + \sum_1^{N-1} (\xi_{n+1}^* \xi_n - 2\xi_{n+1}\xi_n^*)$$
$$+ \beta b^{1/3}\Big(-|\xi_1|^2 - |\xi_N|^2 - \sum_1^N |\xi_n|^2$$
$$+ \sum_1^{N-1} (2\xi_{n+1}^* \xi_n - \xi_{n+1}\xi_n^*)\Big).$$

With β sufficiently small, it is clearly possible to arrange the phases of ξ_n to make ρ grow, while for large β this is not possible.

IV. NUMERICAL SOLUTIONS OF EQ. (2.4)

Two questions cannot be answered by stability analysis: (a) how do solutions to (2.4) develop for $\beta < \beta^*$; (b) are there finite amplitude instabilities for $\beta > \beta^*$. We have examined both questions by integrating (2.4) numerically with $\epsilon = 1$.

It will become evident that the time scale in the nonlinear problem goes as b^n for excitations involving the nth mode as contrasted with the Kolmogorov scale $b^{2n/3}$.[3] In either case, the range of frequencies in the system increases exponentially with N, necessitating a rather small time step to resolve the smallest scales. Fortunately, solutions to our equations tended to what appeared to be their asymptotic form $N \to \infty$ after only a few cascade steps and it was never felt necessary to integrate more than eight equations at a time.

For the integration we used Fehlberg's fourth–fifth-order Runge-Kutta scheme as coded by Shampine and Watts. This code has automatic step size adjustment capabilities which proved particularly useful since a small step was only used when the last few shells were excited. The step size is adjusted to make an error estimate less than a given bound. The bound used was a factor of 10^3 smaller than the value at which any change was noted in the statistics. Such accuracy is superfluous and it will be seen that the nonlinear solutions are generally very stable, and correlation functions are unaffected by a moderate amount of noise with one exception. This property is gratifying since it suggests some insensitivity to the many possible couplings that have been dropped from Eq. (2.4). In particular, spacial diffusion within a shell might be modeled by an appropriately chosen noise source. Integration codes based on Gear's method were not judged necessary for $N \leq 8$.

A further numerical difficulty occurred when α was zero in (2.4). If x_{n-1}, $x_n \sim 0$ while $x_{n+1} \sim 1$ the integration code would proceed in very small steps and x_n would oscillate about zero. Instead of modifying the step size adjustment routine, we took $\alpha > 0$ and verified that correlation functions were independent of α in the range from 10^{-4} to 0.03. To calculate the curves in Fig. 3 required about a second on a C.D.C. 7600 computer once the initial conditions had washed out.

We also experimented with a number of subgrid parametrizations. It was found possible to make the last level scale in accordance with the pattern established in the earlier levels. The results are discussed after those for $\beta > 0$.

A. Results for $\beta = 0$

Generally speaking, the instability of the Kolmogorov solution gave rise to rather well-defined pulses that propagated down the cascade out to $k = \infty$. The period between pulses was set by the time needed to accumulate sufficient energy in the first level. If we had not kept ϵ_n, (2.5), positive and omitted the absolute values in (2.3), as oscillations developed from initial conditions with $x_n > 0$, one level would flip sign and remain negative, causing energy to flow toward large scales and the cascade to collapse.

Approximately one cycle of the motion for $\beta = 0.0$ is shown in Fig. 3. Levels 5–8 are plotted on an expanded scale and are nearly zero prior to the arrival of the pulse from above. The solution rapidly assumes the form of a nearly square pulse after a few cascade steps. It narrows as it goes from level to level, but its height is fixed by energy conservation. "Bursts" of the kind shown, occurred more or less regularly in time. The sys-

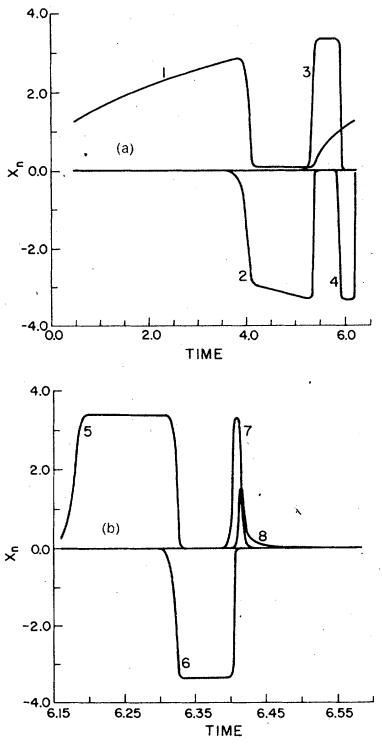

FIG. 3. Approximately one cycle of Eq. (2.4) for $\alpha = 0.01$, $\beta = 0$, $b = 2$, and $N = 8$. Shells 1–4 are plotted in (a) and shells 5–8 in (b) on an expanded scale. The last four shells are zero until the times shown. The origin of time has been shifted to zero. There is no longer any dependence on initial conditions.

tem of equations (2.4) was observed over many burst cycles to be statistically stationary. Equal time correlation functions were computed by time averaging the numerical data. Using just the middle levels, that seem to scale, one finds

$$\langle E_n \rangle \sim b^{-(2/3+\zeta)n}, \quad \zeta = 0.3 \pm 0.04$$
$$\langle \epsilon_n^k \rangle \sim b^{\mu_k n}, \quad \mu_k = k - 1 . \tag{4.1}$$

Only $k = 2, 3$ were checked in the second equation. The errors in the relation for μ_k are small and reflect the errors inherent in the numerical algorithms employed. Somewhat better scaling data was obtained with the subgrid models.

Actually (4.1) can be understood analytically by observing that

$$x_1 = \sqrt{\epsilon t},$$
$$x_n = \delta_n, \quad n \neq 1, m,$$
$$x_m = O(1),$$

where δ_n is infinitesimal, is a quasistationary solution of (2.4) for $\beta = 0$. The propagation of the pulse simply corresponds to transitions between these solutions.

To investigate this process in more detail, solve

$$\dot{x}_n = -b^{n+1} x_{n+1}^2, \quad \dot{x}_{n+1} = b^{n+1} x_n x_{n+1}, \tag{4.2a}$$

with the initial conditions,

$$x_n = (1 - \delta_{n+1}^2)^{1/2}, \quad x_{n+1} = \delta_{n+1} . \tag{4.2b}$$

Equation (4.2a) conserves $x_n^2 + x_{n+1}^2$ and applies so long as $x_n > 0$. It is readily seen that after a time $\sim b^{-(n+1)} |\ln(\frac{1}{2}\delta_{n+1})|$, x_n has reached zero and $x_{n+1} = 1$. The average of E_n over a cycle of the system is just proportional to the lifetime of x_n or

$$\langle E_n \rangle \sim b^{-n} |\ln(\tfrac{1}{2}\delta_{n+1})| . \tag{4.3}$$

The energy transfer is only nonzero while one shell is rising and the preceding one falling. From (4.2)

$$\langle \epsilon_n^k \rangle \sim b^{(k-1)n} . \tag{4.4}$$

Equation (4.4) is independent of δ_m.

Actually x_n does not reach zero when α is positive. For $x_n \lesssim \sqrt{\alpha}$ and $x_{n+1} \sim 1$,

$$\dot{x}_n = -b^{n+1} x_n x_{n+1} / \sqrt{\alpha} .$$

Thus x_n decreases exponentially from a value of order $\sqrt{\alpha}$ for the lifetime of x_{n+1}. The δ_n are related in a rather complicated way and depend on end-point effects (i.e., shells 1 and N). The fact that (4.1) and (4.3) agree, indicates δ_n does not vary greatly with n. It also cannot fall below a value set by the average truncation error. The introduction of significant noise whose rms value varied with n would disrupt the scaling implied by (4.3), but not affect the energy transfer fluctuations.

B. Results for $\beta > 0$

Any small positive β in (2.4) gives rather different results than the $\beta = 0$ case. Again there are a series of pulses that propagate to $k = \infty$ with a repeat period governed by x_1. Figure 4 shows data for $\beta = 0.05$. The pulses were investigated by defining for each $x_n(t)$ a function $f_n(b^n(t^* - t))$ and attempting to collapse all the data onto a single curve by varying t^*, i.e.,

$$x_n(t) = f(b^n(t^* - t)) \equiv f(z) . \tag{4.5}$$

The pulse shape, $f(z)$, derived from levels 3–6 is shown in Fig. 5. The remaining levels are influenced by end-point effects; see Fig. 4. The parameter t^* is the time the energy reaches infinite n or k. It is finite because we are dealing with a local cascade in which the characteristic time decreases by a factor larger than 1 at each step.

It is trivial to demonstrate that any solution to (2.4) of the form $b^{cn} f(b^{dn}(t^* - t))$, with $\int_{-\infty}^{+\infty} \epsilon_n(t) dt$

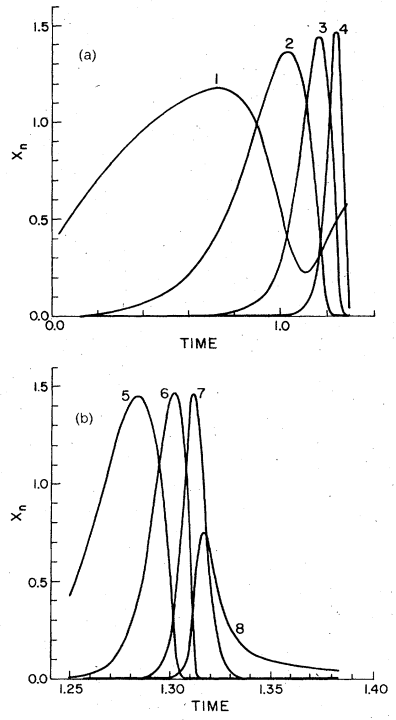

FIG. 4. Approximately one cycle of Eq. (2.4) for $\alpha = 0.01$, $\beta = 0.05$, $b = 2$, and $N = 8$. Other conventions are the same as in Fig. 3.

finite, must have $c = 0$ and $d = 1$. The existence and stability of such a solution have only been demonstrated numerically. The equation for $f(z)$ with $\alpha = 0$ is[14]

$$\frac{df(z)}{dz} = b\left(f^2(zb) + \beta f(z) f(zb)\right) - \left[\beta f^2\left(\frac{z}{b}\right) + f\left(\frac{z}{b}\right) f(z)\right], \tag{4.6}$$

$$f(0) = f(+\infty) = 0 .$$

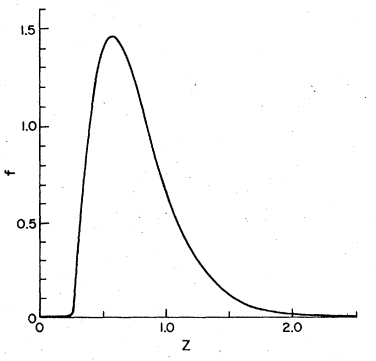

FIG. 5. Pulse shape defined by (4.5) obtained by collapsing x_3, x_4, x_5, and x_6 down to a single curve. The trajectories were obtained by solving (2.4) with $\alpha = 10^{-4}$, $\beta = 0.05$, $b = 2$, and $N = 8$.

For any solution $f(z)$ of (4.6), $cf(zc)$ is also a solution for any constant c.

Equation (4.6) possesses at least two distinct solutions in the neighborhood of infinity. The first is expressed as a power series in $z^{-1/3}$ that Bell has shown does not match onto any solution of (4.6) for small z.[14] The second is of the form

$$f(z) = \frac{b^{2\gamma-2}}{\beta} e^{-z^{\gamma}} \left(\gamma z^{\gamma-1} - \frac{\gamma - 1}{z(2b^{\gamma} - 1)} + O(z^{-\gamma-1})\right), \tag{4.7}$$

$$\gamma = \ln 2 / \ln b .$$

Neither higher-order terms nor the convergence of the series in z have been checked. However, the exponential factor has been verified numerically for $b = 2$ and 1.6. For small z, there is a solution to (4.6) that appears to go as

$$f(z) = b^{2\gamma+1} e^{-z^{-\gamma}} \left(\gamma z^{-\gamma-1} - \frac{\gamma + 1}{z(2b^{\gamma} - 1)} + O(z^{\gamma-1}1)\right). \tag{4.8}$$

This form was also checked numerically, but now α is expected to influence the result since as $z \to 0$ using (4.8), $f^2(z) \ll \alpha f^2(bz)$. It is uncertain whether a solution of the form (4.5) to (2.4) exists for $\alpha > 0$. The difficulties, if any, are confined to small z when f itself is very small. Equation (4.7) is not affected by α and numerical data for $\alpha = 10^{-2}$ and 10^{-4} fit (4.5) perfectly.

Provided only that $\int_0^{\infty} f^m(z)dz$ for $m \geq 2$ is finite, (4.5) implies,

$$\langle E_n \rangle \sim b^{-n}, \quad \langle E_n^k \rangle \sim b^{n(k-1)} . \tag{4.9}$$

There is no longer any ambiguity about the energy exponent.

We believe that a computation with 8 shells gives a true indication of the asymptotic ($N \to \infty$) form of solutions to (2.4). With only four shells, the pulses are already quite distinct and have the same form as for $N = 8$, Fig. 6.

A series of numerical runs have been made with $\alpha = 0.01$, $b = 2$, $N = 8$, and β variable to examine

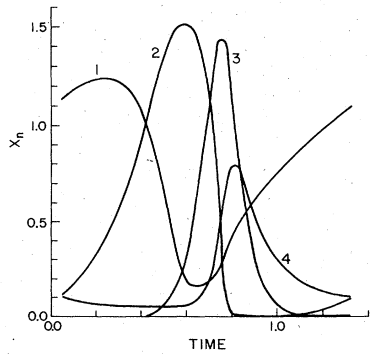

FIG. 6. Shells 1–4 from Eq. (2.4) solved with $\alpha = 0.01$, $\beta = 0.05$, $b = 2$, and $N = 4$. Note the resemblance to Fig. 4.

how the nonlinear solutions change near $\beta^* = 0.145\,10$, the point of linear stability. For $\beta = 0.1$, the first few levels oscillated about their Kolmogorov values, but the oscillations increased with n so that the last few levels are very similar to the $\beta = 0.05$ results. A qualitatively similar picture was found for $\beta = 0.14$ except that the oscillations were of smaller magnitude and the pulses required more shells to develop. It is now less clear that (4.5) represents the limiting solution as $N \to \infty$. With $\beta = 0.15$ and 0.3 no finite amplitude instabilities of the Kolmogorov solution were found. For the smaller value of β, however, it took some time for the solutions of (2.4) to settle down to (3.1). Pulselike solutions developed during the relaxation. Small perturbations to (2.4) which do not admit the scaling solution (3.1) favor the persistence of the pulses.

C. Subgrid models

The stability properties of the first subgrid parametrization (2.7a) were discussed in Sec. II. For a number of values of β and $N = 8$, we attempted to adjust τ in (2.7a) to make the last level fit (4.5). One could equally well have worked with only six equations and attempted to fit the sixth level to the $N = 8$ data. The best results for $\beta = .05$ are shown in Fig. 7. Shells 1–4 were unaffected by the subgrid model and were not redrawn. A number of runs were also made in the second unstable region of Fig. 2 for $\tau = 0.013$. Again, only the last level was affected and although it looks different than Fig. 7, it is not in better agreement with (4.5).

The second subgrid model was somewhat more successful. The lag time τ was again varied to make the last level scale with the preceding ones.

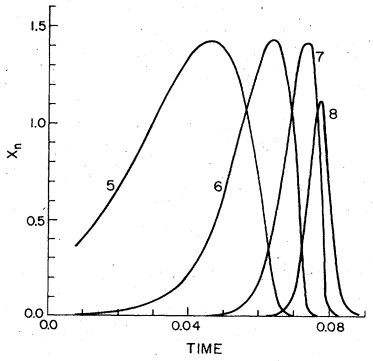

FIG. 7. A solution of (2.4a), (2.4b), and (2.7a) for $\alpha = 0.01$, $\beta = 0.05$, $b = 2$, $N = 8$, and $\tau = 0.0031$. The lag τ has been adjusted as best as possible to make the last shell scale with the preceding ones. The first four shells are unchanged from Fig. 4(a), and only levels 5–8 are redrawn.

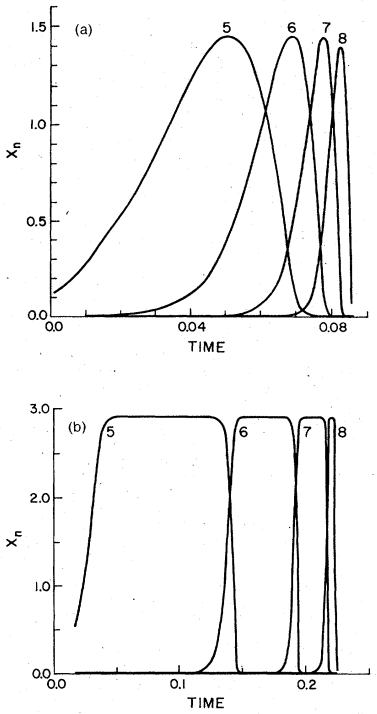

FIG. 8. Test of the subgrid model, Eq. (2.8), combined with (2.4a), (2.4b) and (2.4d) for $\alpha = 0.01$, $b = 2$, and $N = 8$. In (a) $\beta = 0.05$, $\tau = 0.004$ and in (b), $\beta = 0$, $\tau = 0.007$. The lag times have been adjusted to make the last level scale. Shells 1–4 are unchanged from Figs. 4(a) and 3(a). Only the last four shells are plotted.

The results for $\beta = 0.05$ are shown in Fig. 8(a). Actually the agreement is not perfect, since the last level does not cut off as sharply as it should. This has a negligible effect on both the average energy and ϵ_8. Figure 8(b) shows the results for $\beta = 0.0$ that should be compared with Fig. 3(b).

A stability analysis has not been done with (2.8) in place of (2.4c), but a number of runs have been made with increasing β. Again the trend is for the lagged feedback to favor the Kolmogorov solution. With β in the range 0.07–0.08, $\alpha = 0.01$, and the same lag τ as was used to generate Fig. 8; the bursts became irregular in the first few shells but more pronounced in the latter ones. For $\beta \gtrsim 0.09$, the Kolmogorov solution reappeared, but with a small amount of noise because $\beta^* > \beta$. There is also the suggestion for $\beta = 0.05$, that increasing τ leads to stability, i.e., no pulses, and then instability again, Fig. 2.

V. CONCLUSION

It is commonly thought, though we know of no definitive models, that the measured intermittency spectra are due to the convection of coherent structures variously associated with ribbons, tubes or

sheets of vorticity.[8,9] Such ideas presumably are motivated by experience with laminar flows while our models are statistical from the beginning. Is there any reconciliation?

We suspect, that to obtain agreement with the inertial range spectra for the velocity structure functions[5] $\langle[v(r)-v(0)]^n\rangle$, it is necessary to hypothesize some distribution of thicknesses for the imbedded structures. It would seem difficult, for instance, to get the correct scaling behavior of higher-order correlation functions from a crinkled sheet of thickness the Kolmogorov microscale. If some small patch of vorticity of size λ in the inertial range had a much greater life time against stretching or crinkling than a Kolmogorov estimate based on λ would imply by virtue of its incorporation in a larger structure, then our model is incorrect. The model outlined in the introduction describes correctly vortex stretching at least locally.[2] It would correctly predict on average the crinkling and stretching of some small segment of a vortex sheet which would appear as the transfer of energy into higher bands.

Single point measurements cannot identify structures and by comparison with these experiments the model of Ref. 2 does quite well. The only multipoint experiments we know, that indicate the presence of small-scale structures in approximately homogeneous isotropic turbulence, are those of Kuo and Corrsin.[8] A certain amount of modeling, which did not fit experiment for scales larger than several times the microscale, was required, however, to interpret the results.

The model outlined in the introduction and a model derived for two-dimensional turbulence by Lorenz both employ a uniform number of modes per band to simplify the theory.[15] A number of distinctions between the two models should be emphasized. Most important is the physical meaning of the degrees of freedom; ours are local in both real space and Fourier space. Lorenz collapsed the modes in a wave number band down to a discrete subset. The sum of the squared-velocity magnitudes at these wave vectors should represent the volume averaged energy in that wave-number band. For stationary turbulence, this quantity is independent of time. Similar remarks apply to the models constructed by Obukhov,[16] Bell and Nelkin,[14,17] and Desnyansky and Novikov[10] which bear a superficial resemblance to (2.4). With respect to a wave packet basis, we are able to say physically that retaining only a constant number of modes per band neglects diffusion in real space, i.e., coupling between different boxes in the same shell. We know of no physical characterization of the effects missed by wave vector sampling methods.

It is frequently thought necessary that a turbulence model should achieve the same equipartition solution as do the suitably truncated Navier-Stokes equations when dissipation is turned off.[18] Our model fails this test for two reasons: (i) The number of modes does not increase with k; (ii) Equation (2.4) does not satisfy Liouville's theorem. The first deficiency is true for any sampling method applied to the equations of motion and we regard it as unimportant. The second difficulty is a consequence of using variables that represent the mean amplitude of a number of modes and does not disqualify our model. We suspect a similar problem would arise in solving the direct interaction approximation numerically in a homogeneous isotropic system,[18] if one first discretized in wave number and then introduced a sufficient number of auxiliary variables to make the retarded interactions local in time. A system of the form

$$\dot{x}_i = f_i(\{x_j\})$$

would result which would probably also violate Liouville's theorem.

All previous theoretical work on intermittency that we are aware of for homogeneous isotropic turbulence is kinematic in that one exploits symmetries and conservation laws or makes physical assumptions about equal time correlation functions rather than solving equations in time.[19,20] It is interesting to note that the exponents in (4.9) satisfy a relation first proposed by Mandelbrot and given a more physical interpretation by subsequent authors. Mandelbrot proposed,

$$\zeta = \tfrac{1}{3}\mu_2\,, \quad \mu_k = \mu_2(k-1)\,, \tag{5.1}$$

with

$$\mu_2 = 1$$

required to satisfy (4.9). This relationship is a consequence of the simplest possible assumption for the probability distribution of a local velocity amplitude or eddy velocity x_n in shell n that goes beyond a $\frac{5}{3}$ law,

$$\mathcal{P}(x_n) = (1-b^{-en})\delta(x_n) + b^{fn}p(b^{gn}x_n)\,. \tag{5.2}$$

The first constraint imposed on the three parameters e, f, and g is that $\mathcal{P}$ integrate to 1. For the second constraint, the energy transfer rate between shells n and $n+1$ is estimated as $b^n x_n^3$ and its average in a stationary system assumed independent of n. The three parameters in (5.2) can now be expressed in terms of the single variable, μ_2, that appears in (5.1),

$$e = \mu_2\,, \quad f = \tfrac{1}{3} - \tfrac{4}{3}\mu_2\,, \quad g = \tfrac{1}{3}(1-\mu_2)\,.$$

The large number of modes required to span a reasonable range of wave numbers and the in-

creasing characteristic frequencies in small scales combine to effectively prohibit high-Reynolds-number simulations. The former problem is the principal constraint in three dimensions and the one wave vector sampling techniques are designed to overcome.

Experiments have tended to confirm Kolmogorov's ideas that small scale properties such as the exponents in (4.9) are independent both of geometry and initial conditions. One is then lead to ask if an exponentially increasing number of modes in successive shells are all really needed to calculate such "universal properties," or whether an approximation that greatly reduces the number of degrees of freedom could in principle be exact. More generally, are there any properties that are universal, i.e., the same for all equations in a given class or perhaps just with respect to some domain of parameters in a given equation. Even the weaker form of universality would be of great assistance since it would mean that the parameters entering a model such as the one given here do not have to be calculated from the Navier-Stokes equations.

Equations (2.4) probably possess the weak form of universality. The physically relevant parameter space of α, β, b can be divided into two regions. In one, the exponents in (5.1) apply while in the other Kolmogorov's $\frac{5}{3}$ law obtains with no fluctuations in the energy transfer. Near the boundary between the two regions, our numerical calculations do not preclude other exponents or even the absence of scaling laws altogether.

To investigate the stronger form of universality, a number of models with two modes per band but in other respects similar to (2.4) were integrated. The second degree of freedom permitted the actual energy transfer to lag the value given in (2.5). A preliminary search through the enlarged parameter space has revealed only an intermittent solution obeying (5.1) and a static Kolmogorov solution.

One should also ask if scaling exponents will change if intrashell diffusion and coupling between second-neighbor and more-distant shells are included. Will there again exist regions of parameter space where exponents do not vary? These questions are just beginning to be studied.

The second potential difficulty for numerical simulations and the limiting factor in wave vector sampling methods is the increasing characteristic frequency with N. To solve (2.4) with $N=60$ and a constant time step would require about 10^{10} years of computation on a C.D.C. 7600 computer. For this reason we were unable to investigate if solutions to (2.4) scaled near the boundary between the intermittency region and the $\frac{5}{3}$ region.

The increasing frequency of small scales is what generates their statistical independence of the larger scales. Physically, the obvious method of solution is to let the system evolve until the smallest scales have settled down to a stationary state. They could then in principle be removed and their effects on larger scales parametrized. The step size could then be increased and the same procedure applied to the next group of modes. The practical success of such a scheme is favored by a local cascade and an inertial range with no intrinsic length scales. Numerous variants of the above method are easily constructed, but the physics is always the same.[21] Models such as (2.4) incorporate a sufficient number of qualitative properties of the Navier-Stokes equations at high Reynolds numbers that they may prove a useful tool in evaluating such computations.

ACKNOWLEDGMENTS

The author benefited from a number of conversations with T. Bell, M. Nelkin, S. Corrsin, and S. Orszag. He is indebted to Bell and Nelkin for communicating their results prior to publication. This work was done during a visit to the National Center for Atmospheric Research, which is sponsored by the National Science Foundation.

APPENDIX

A plausible and simple representation of (2.4) for $\alpha=0$ in the limit $b\to 1, N\to\infty$ can be constructed as follows. Define

$$y = n \ln b$$

and

$$x_n(t) = w(y,t),$$

and let

$$x_{n\pm1}(t) = w \pm \ln b \frac{\partial w}{\partial y}. \tag{A1}$$

To first order in $\ln b$, (2.4) becomes

$$\frac{\partial w}{\partial y} = -(1+\beta)\ln b\, e^{y}\left(|w|w + 3|w|\frac{\partial w}{\partial y}\right). \tag{A2}$$

In substituting (A1), we have assumed that x_n and $x_{n\pm1}$ have the same sign. This need not be strictly true, but (A2) will be shown to have the correct conservation laws. An equation for the energy, $E(y,t)=\frac{1}{2}w^2$,

$$\frac{\partial E}{\partial t} = -(1+\beta)\ln b \frac{\partial}{\partial y}(e^{y}|w|w^2),$$

implies an energy transfer to higher wave numbers of

$$\epsilon(y,t) = (1+\beta)\ln b\, e^{y}|w|w^2.$$

Thus the continuum limit of (3.1),

$$w = ce^{-y/3},$$

satisfies (A2).

Equation (A2) assumes a more familiar form with the substitutions,

$$w(y,t) = e^{-y/3}v(z,t), \quad z = e^{-2y/3},$$

namely,

$$\frac{\partial v}{\partial t} = 2(1+\beta)\ln b\,|v|\,\frac{\partial v}{\partial y}. \tag{A3}$$

To the limited extent we have used (A3) to analyze solutions of (A2), they do not resemble those found for (2.4) with $b > 1$. In addition, continuing a model with only nearest-neighbor interactions to the limit $b \to 1$ is rather unphysical.

---

[1]M. Rosenblatt and C. Van Atta, *Statistical Models and Turbulence*, (Springer Verlag, New York, 1971).

[2]E. D. Siggia, Phys. Rev. A 15, 1730 (1977).

[3]L. D. Landau and E. M. Lifshitz, *Fluid Dynamics* Addison-Wesley, Reading, Mass., 1959).

[4]R. H. Kraichnan, J. Fluid Mech. 62, 305 (1974).

[5]C. Van Atta and J. Park, in Ref. 1.

[6]R. H. Kraichnan, J. Atmos. Sci. 33, 1521 (1976).

[7]Wave packets, without any superimposed Fourier modes, proved to be a useful device for "thinning" the degrees of freedom in early renormalization-group calculations. See K. G. Wilson and J. Kogut, Phys. Rep. C 12, 77 (1974).

[8]A. Y.-S. Kuo and S. Corrsin, J. Fluid Mech. 50, 285 (1971). A. Y.-S. Kuo and S. Corrsin, J. Fluid Mech. 56, 447 (1972).

[9]P. G. Saffman, in *Topics in Nonlinear Physics*, edited by N. Zabusky (Springer Verlag, New York, 1968), p. 485.

[10]V. N. Desnyansky and E. A. Novikov, Prikl. Mat. Mekh. 38, 507 (1974); Izv. Adad. Nauk. SSSR, Fiz. Atmos. Okeana [Atmos. Oceanic Phys. 10, 127 (1974)].

[11]J. W. Deardorff, J. Fluids Eng., 429 (1973).

[12]Path integrals were first used in the context of Brownian motion by N. Wiener; see M. Kac, Bull. Am. Math. Soc. 72, 52 (1966).

[13]R. P. Feynman and A. R. Hibbs, *Quantum Mechanics and Path Integrals* (McGraw Hill, New York, 1965).

[14]Similar equations have been investigated by T. Bell and M. Nelkin, J. Fluid Mech. (to be published).

[15]E. N. Lorenz, J. Fluid Mech. 55, 545 (1972).

[16]A. M. Obukhov, Atmos. Oceanic Phys. 7, 471 (1971).

[17]T. Bell and M. Nelkin, Phys. Fluids 20, 345 (1977).

[18]See, for instance, the article by J. R. Herring and R. H. Kraichnan, in Ref. 1.

[19]B. Mandelbrot, in *Proceedings Journées Mathématique sur la Turbulence*, edited by R. Teman (Springer Verlag, New York, 1976).

[20]M. Nelkin, Phys. Rev. A 11, 1737 (1975); U. Frisch, P. L. Sulem, and M. Nelkin, J. Fluid Mech. (to be published); M. Nelkin and T. Bell (private communication).

[21]H. Rose, J. Fluid Mech. (to be published).